ORIGINAL PAPER

Optimization of the free vibrations of doubly-curved sandwich panels using the artificial bee colony optimization algorithm

Zhaofang Du[1]

Abstract

This study examines the optimization of double-curved sandwich panels containing composite layers and magnetorheological (MR) fluid cores to determine the optimal parameters that influence free vibration. The bee optimization algorithm was applied to minimize the mass and maximize the first modal loss factor. Additionally, the improved high-order theory (IHOT) and extended Hamilton's principle were applied for the first time to extract the motion equations of the panel. The layers and core thickness, the fibers angle, and magnetic intensity have been assumed to be optimization parameters. For the first time, the technique for order of preference by similarity to ideal solution (TOPSIS) technique has been applied to obtained the optimal design points from a set of optimal points. This indicates that in a similar situation regarding dimensions and mass, doubly-curved panels exhibit a greater modal loss factor than single-curved panels. The results of the bee and particle swarm optimization algorithms demonstrate that the bee algorithm provides the modal and mass loss factors 50% and 30% better than the particle swarm algorithm, respectively. As a result, this method is highly recommended for analyzing such issues.

Keywords Optimization · Sandwich panel · Loss factor · Bee colony algorithm · Pareto front

1 Introduction

Composite structures and panels are modern structures possessing a considerably high strength-to-weight ratio due to their unique properties (Pekbey et al. 2012; Maleki and Toygar 2019; Hoseinzadeh et al. 2023; Maleki et al. 2022; Niu et al. 2022; Li et al. 2022). In general, low weight, resistance to a specific load, and multi-purpose ability have increased the usage of these panels (Vinyas 2020). A sandwich structure comprises two thin yet strong layers that coat a flexible, soft, and moderately thick core. The layers are frequently made of thin and strong metal or multi-layered panels. The core of these structures is typically composed of light polymers, foams, or honeycomb structures (Makweche and Dundu 2022; San Ha and Lu 2020; Khosravi 2022; Toygar et al. 2019).

Overall, fluids whose characteristics change with the alteration of the magnetic field are called magnetorheological fluids. These materials are widely utilized to control structures owing to their swift time response (Kolekar et al. 2019). Moreover, there is a significant change in the hardness and loss properties of these fluids. Also, these fluids are ideal for controlling large-amplitude vibrations (Nagiredla et al. 2022; Joladarashi et al. 2022; Momeni and Zabihollah 2023). Among the recent studies on MR fluid is the work of Selvaraj et al. (Selvaraj et al. 2023). They investigated the optimum placement of the MR layers to maximize the loss factor of a sandwich beam. In addition, Lotfan et al. (2021) have introduced a general framework for the formulation and calculations of the dynamic analysis of the shell and the multilayered doubly-curve sheet with a medium thickness. Optimizing is an important and decisive part of the structural design process. Optimizing methods allows designers to produce better designs and save time and money. Boddeti et al. (2020) analyzed the optimal design with discrete variables stiffness of sandwich sheets. Gao et al. (2019) also optimized corrugated-core sandwich panels by minimizing two objective functions, including weight and structure deviation. Cai et al. (2021) examined a general procedure for optimizing sandwich sheets to minimize the impacts of explosive loading. Ly et al. (2022a) developed a neural network-nondominated sorting genetic algorithm II

✉ Zhaofang Du
  lightmoon88@163.com

1   Henan Industry and Trade Vocational College, Zhengzhou 450053, Henan, China

approach to optimize laminated carbon nanotube-reinforced composite quadrilateral panels.

Using magneto-electro-elastic panels combined with active damping, Nguyen-Thoi et al. (2022) examined vibration analysis and optimal control. Their study examines the influence of porous distribution and boundary conditions on the dynamic response of the plate as well as the optimal control solution. For hybrid damping vibration control of laminated composite plates, Ly et al. (2022b) utilized the zig-zag theory. The influence of magnetic field and materials on the vibrations of MR-laminated beams was studied by Ly et al. (2022c) and Momeni and Zabihollah (2023). To construct the sandwich MR-laminated beam, materials, including carbon fiber, E-glass, and Kevlar, have been used as base materials. For different boundary conditions of MR fluid sandwich beams, Nagiredla et al. (2023) determined the influence of magnetic field strength, length, and thickness on loss factor, deflection, and frequencies. Sharif et al. (2022) manufactured and experimentally analyzed beams with a metal face plate and an elastomer in a honeycomb core. Based on the results of the experiment, it was established that frequencies, amplitudes, and damping ratios of panels with MR honeycomb cores shifted with an increase in an induced magnetic field. Under high-temperature conditions, Mirzavand Borojeni et al. (2022) investigated the influence of magnetoelastic load and temperature on the dynamics of an elastomer beam. Based on elastic foundations and corrugated composite sandwich plates filled with MR elastomer, Zhao et al. (2023) investigated their dynamic behavior. A comparison of numerical results indicates that the performance of the structure is improved when the magnetic field intensity, boundary stiffness, and elastic foundation are increased. Based on the study by Zheng et al. (2023), predictions of nth-order derivatives of dynamics and loss factors for a shell composed of an MR core and composite face layers. Sahu et al. (2022) investigated the dynamics of the MR sandwich plate and found increasing modal loss factors and frequencies when the magnetic field is applied.

The main objective of this work is to obtain optimal values of effective parameters on the free vibrations of the panel for single- and multi-objective optimization of doubly-curved panels with laminated faces and MR core to minimize the mass and maximize the loss factor by the bee algorithm. Sandwich panel studies in this research have simple support conditions. Using the high-order theory of sandwich panels for the first time, the equations of motion governing the doubly-curved sandwich panel with MR core and Hamilton's principle were extracted to determine the objective optimization functions for the system based on the IHOT of sandwich panels. Following the extraction of the equations of motion that govern the system, comparing them to similar results, and ensuring that the extracted equations are correct and reliable, a single-objective and multi-objective
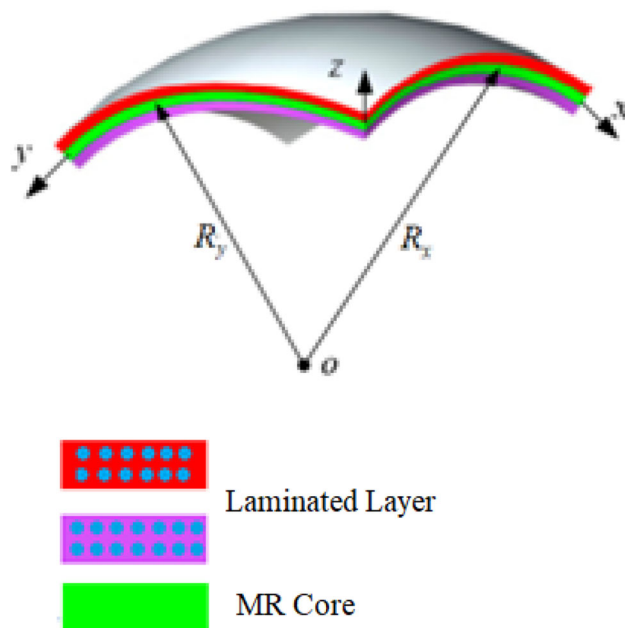

Fig. 1 Doubly-curved sandwich panel geometry with composite layers and MR core

optimization of the panel has been performed utilizing this valid model. As a next step, the layer thickness, the thickness of the core, the fiber angle, and the magnetic field intensity were considered optimization variables. Single-objective optimization involves finding the intensity of the magnetic field and the optimal thickness for the layers to improve the panel's vibrations. Furthermore, minimizing the sheet's mass is considered in multi-objective optimization in addition to the vibration behavior criterion.

2 Formulation

Considering that the face layers thickness is usually thin, therefore the theory of first-order shear deformation theory will be accurate. On the other hand, due to the greater thickness of the core, it is better to use high-order theories. Based on this, in the present research, to improve the accuracy of the mathematical model, surface layers are modeled using the FSDT, and the thick core is modeled using the high-order theory. The IHOT of the sandwich panel was utilized to obtain the motion equations of the system. Based on this theory, the FSDT theory has been used for the layers' composite panel. Furthermore, for the core, the polynomial expression of the displacements based on the displacements of the high-order model presented by Frostig et al. (Frostig and Thomsen 2004) is used. Subsequently, using the minimum potential energy principle, governing equations have been extracted. The geometry of a doubly-curved sandwich panel with MR core and composite (laminated) layers is shown in Fig. 1.

Based on FSDT, v, u, and w displacements of layers in the y, x, and z directions, assuming linear displacements, are as:

$$u_i(x, y, z, t) = u_0^i(x, y, t) + z\psi_x(x, y, t)$$
$$v_i(x, y, z, t) = v_0^i(x, y, t) + z\psi_y(x, y, t)$$
$$w_i(x, y, z, t) = w_0^i(x, y, t), \quad i = T, B \tag{1}$$

where t represents time, ψ_x is the normal rotation components around the x axes, and ψ_y is the normal rotation components around the y axes. u_0^i, v_0^i and w_0^i are displacements in the direction of the x- and y-axes and the vertical deformation of the layers. T and B represent the top and bottom surfaces of the panel, respectively.

Based on the Frostig model (Frostig and Thomsen 2004), displacement for the core are as:

$$u_c(x, y, z, t) = \left(1 + \frac{z}{R_x}\right) u_0^c(x, y, t) + z_c^3 u_3^c(x, y, t)$$
$$+ z_c^2 u_2^c(x, y, t) + z_c u_1^c(x, y, t) \tag{2}$$

$$v_c(x, y, z, t) = \left(1 + \frac{z}{R_y}\right) v_0^c(x, y, t) + z_c^3 v_3^c(x, y, t)$$
$$+ z_c^2 v_2^c(x, y, t) + z_c v_1^c(x, y, t) \tag{3}$$

$$w_c(x, y, z, t) = z_c^2 w_2^c(x, y, t) + z_c w_1^c(x, y, t) + w_0^c(x, y, t) \tag{4}$$

where u_k^c and v_k^c stand in-plane displacements and w_k^c ($k = 0$, 1, 2) is the vertical displacements. R_x and R_y represent the curvature of the panel in *the y*- and *x*- plane, respectively. This research assumes that the layers are ideally attached to the core. As a result, all of the upper layer and the core displacement components are equal at the interface. So, assuming full bending among the layers and the core, the compatibility equation in the bottom and top connection of layers and core is obtained as:

$$u_c(z = z_c) = u_0^i + \frac{1}{2}(-1)^k h_i \psi_x^i$$
$$v_c(z = z_c) = v_0^i + \frac{1}{2}(-1)^k h_i \psi_y^i \tag{5}$$
$$w_c(z = z_c) = w_0^i$$

where h_i is the thickness of the ith layer.

MR has linear viscoelastic properties before yielding, so its shear modulus is mixed and depends on its magnetic field intensity. In this research, the relationship proposed for the connection between MR magnetic field intensity and mixed shear modulus is employed (Srinivasa et al. 2020). The mixed shear modulus for viscoelastic materials is defined as

(Rajamohan et al. 2010):

$$Q = Q' + iQ'' \tag{6}$$

where Q' and Q'' represent storage modulus and loss modulus, respectively, and for MR, it is a polynomial function of the intensity of the magnetic field B as:

$$Q' = -3.3691B^2 + 4.9675 \times 10^3 B + 0.873 \times 10^6 \tag{7}$$

$$Q'' = -0.9B^2 + 0.8134 \times 10^3 B + 0.1865 \times 10^6 \tag{8}$$

Finally, by replacing the displacement fields and also the relations of the layers' stress in the relations of the potential and kinetic energy variation using Hamilton's principle (Fallah and Arab Maleki 2021; Pourreza et al. 2022, 2021; Nasrabadi et al. 2022) and the basic principle of the calculus of variations, the motion equations for the doubly-curved sandwich panel with the MR core are acquired. Therefore, after some algebraic manipulation, the motion equations obtained as:

$$\left(\frac{1}{3}\frac{\partial^2 u_0^T}{\partial t^2} + \frac{1}{6}\frac{\partial^2 u_0^B}{\partial t^2} + \frac{1}{12}\frac{\partial^2 w_0^B}{\partial x \partial t^2} - \frac{1}{6}\frac{\partial^2 w_0^T}{\partial x \partial t^2}\right) M_c$$
$$- \frac{\partial N_{xx}}{\partial x} - \frac{\partial N_{xy}}{\partial y} + \frac{\partial^2 u_0^T}{\partial t^2} M_t - \left(\psi_x^T + \psi_x^B\right) = 0 \tag{9}$$

$$\left(\frac{1}{3}\frac{\partial^2 v_0^T}{\partial t^2} + \frac{1}{6}\frac{\partial^2 v_0^B}{\partial t^2} + \frac{1}{12}\frac{\partial^2 w_0^B}{\partial y \partial t^2} - \frac{1}{6}\frac{\partial^2 w_0^T}{\partial y \partial t^2}\right) M_c$$
$$- \frac{\partial N_{yy}}{\partial y} - \frac{\partial N_{xy}}{\partial x} + \frac{\partial^2 v_0^T}{\partial t^2} M_t - \left(\psi_y^T + \psi_y^B\right) = 0 \tag{10}$$

$$\left(-\frac{1}{12}\frac{\partial^4 w_0^T}{\partial y^2 \partial t^2} + \frac{1}{12}\frac{\partial^3 u_0^B}{\partial x \partial t^2} + \frac{1}{24}\frac{\partial^4 w_0^B}{\partial x^2 \partial t^2} + \frac{1}{6}\frac{\partial^3 u_0^T}{\partial x \partial t^2}\right.$$
$$+ \frac{1}{6}\frac{\partial^2 w_0^B}{\partial t^2} - \frac{1}{12}\frac{\partial^4 w_0^T}{\partial x^2 \partial t^2} + \frac{1}{6}\frac{\partial^3 v_0^T}{\partial y \partial t^2}$$
$$\left. + \frac{1}{24}\frac{\partial^4 w_0^B}{\partial y^2 \partial t^2} + \frac{1}{12}\frac{\partial^3 v_0^B}{\partial y \partial t^2} + \frac{1}{3}\frac{\partial^2 w_0^T}{\partial t^2}\right) M_c$$
$$- \left(\frac{\partial^4 w_0^T}{\partial x^2 \partial t^2} + \frac{\partial^4 w_0^T}{\partial y^2 \partial t^2}\right) I_{mt} \frac{1}{2}\left(\frac{\partial \psi_x^T}{\partial y} + \frac{\partial \psi_y^T}{\partial x}\right)$$
$$- 2\frac{\partial^2 M_{xy}}{\partial x \partial y} - \frac{\partial^2 M_{yy}}{\partial y^2} - \frac{\partial^2 M_{xx}}{\partial x^2}$$
$$- Q\left(\frac{\partial^2 N_{xx}}{\partial x^2} + \frac{\partial^2 N_{yy}}{\partial y^2}\right) = 0 \tag{11}$$

$$\left(\frac{1}{3} \frac{\partial^2 u_0^B}{\partial t^2} + \frac{1}{6} \frac{\partial^2 u_0^T}{\partial t^2} + \frac{1}{12} \frac{\partial^2 w_0^T}{\partial y \partial t^2} - \frac{1}{6} \frac{\partial^2 w_0^B}{\partial y \partial t^2} \right) M_c \quad (12)$$

$$- \frac{\partial N_{yy}}{\partial y} - \frac{\partial N_{xy}}{\partial x} + \frac{\partial^2 u_0^B}{\partial t^2} M_t - \left(\psi_y^T + \psi_y^B \right) = 0$$

$$\left(\frac{1}{3} \frac{\partial^2 v_0^B}{\partial t^2} + \frac{1}{6} \frac{\partial^2 v_0^T}{\partial t^2} + \frac{1}{12} \frac{\partial^3 w_0^T}{\partial x \partial t^2} - \frac{1}{6} \frac{\partial^3 w_0^B}{\partial x \partial t^2} \right) M_c \quad (13)$$

$$- \frac{\partial N_{xx}}{\partial x} - \frac{\partial N_{xy}}{\partial y} + \frac{\partial^2 v_0^B}{\partial t^2} M_t - \left(\psi_x^T + \psi_x^B \right) = 0$$

in which N_{yy}^j, N_{xx}^j and N_{xy}^j remain stress resultants in the transverse and longitudinal directions, and the in-plane shear stress resultant; M_{yy}^j, M_{xx}^j and M_{xy}^j stand bending moment in transverse and longitudinal directions and the torsion moment, respectively. These parameters are obtained as:

$$\begin{bmatrix} N_{xx}^j & M_{xx}^j \\ N_{yy}^j & M_{yy}^j \\ N_{xy}^j & M_{xy}^j \end{bmatrix} = \sum_{i=1}^{3} \int_{z_i}^{z_{i+1}} \left\{ \begin{array}{c} \sigma_x^j \\ \sigma_y^j \\ \sigma_{xy}^j \end{array} \right\} (1, z) \mathrm{d}z \quad (14)$$

It can be observed that the following answers can meet the simple support boundary conditions.

$$\begin{bmatrix} u_0^j \\ v_0^j \\ w_0^j \\ \psi_x^j \\ \psi_y^j \\ u_k^c \\ v_k^c \\ w_k^c \end{bmatrix} = \sum_{n=1}^{\infty} \sum_{m=1}^{\infty} \begin{bmatrix} \cos(\alpha_m x) \sin(\beta_n y) U_{0mn}^j(t) \\ \sin(\alpha_m x) \cos(\beta_n y) V_{0mn}^j(t) \\ \sin(\alpha_m x) \sin(\beta_n y) W_{0mn}^j(t) \\ \cos(\alpha_m x) \sin(\beta_n y) \psi_{xmn}^j(t) \\ \sin(\alpha_m x) \sin(\beta_n y) \psi_{ymn}^j(t) \\ \cos(\alpha_m x) \sin(\beta_n y) U_{kmn}^c(t) \\ \sin(\alpha_m x) \cos(\beta_n y) V_{kmn}^c(t) \\ \sin(\alpha_m x) \sin(\beta_n y) W_{kmn}^c(t) \end{bmatrix},$$

$$\alpha_m = \frac{m\pi}{L_x}, \quad \beta_n = \frac{n\pi}{L_y} \quad (15)$$

where m and n are the wave numbers. Substituting Eq. (15) in the motion equations of and then using the weighted residual method, and Galerkin method (Maleki and Mohammadi 2017; Rezaee and Maleki 2015; Rezaee and Arab Maleki 2019), the governing equations are obtained as a system of coupled ODE as:

$$[\mathbf{M}]\{\ddot{\mathbf{d}}\} + [\mathbf{K}]\{\mathbf{d}\} = \{\mathbf{0}\} \quad (16)$$

where $\{\mathbf{d}\} = \{U_{0mn}^j, V_{0mn}^j, W_{0mn}^j, \psi_{xmn}^j, \psi_{ymn}^j, U_{0mn}^c, V_{0mn}^c, W_{0mn}^c\}^T$. Instead of a set of differential equations, Eq. (16) produces a set of homogeneous algebraic equations. As a result, PDEs are substituted by an eigenvalue problem, stiffness and mass matrix, in which eigenvalue equals the square of eigenfrequency, and eigenvectors are the series constants for each m and n. Consequently, the last two equations of motion, which describe the compatibility conditions

in the longitudinal and transverse directions at the lower face–core interface, do not contain any inertial terms. So, the stiffness matrix can be reduced to the same dimension as the mass matrix by a factor of 6. Therefore, for specified values of m and n, the eigenvalue problem yields only six eigenfrequencies. Eventually, supposing free vibrations, and also considering that the MR shear modulus is mixed and is in terms of the magnetic field intensity, an eigenvalue problem with complex eigenvalues will be acquired from which the system frequencies, ω, and the loss factor, η, for different vibration modes, can be obtained as:

$$\omega = \sqrt{\mathrm{Re}(\overline{\omega}^2)}, \quad \eta = \frac{\mathrm{Im}(\overline{\omega}^2)}{\mathrm{Re}(\overline{\omega}^2)} \quad (17)$$

3 Optimization

The bee optimization algorithm is a collective intelligent search algorithm for solving optimization problems initially developed in 2006 (Pham et al. 2006). This algorithm simulates the behavior of bee groups searching for food in nature. This algorithm can optimize single or multi-objective problems. The special features of this method make it impossible to consider it a simple, random, and conventional searcher or nature imitation without any reason. The flow chart of the main stages of the bee algorithm is summarized in Fig. 2. The sources (Kamaruddin and Abd Latif 2019) provide more details about this algorithm. This algorithm depends on several parameters the user must specify before starting the algorithm (Table 1).

The objective function in this research is the loss factor ($f(X) = \eta$) for the single-objective mode and the modal loss factor and the weight ($f(X) = \eta, \ m(X)$) for the two-objective mode. The design parameters include the magnetic field intensity (B), the fibers angles, the composite layers' thickness, and the core's thickness. The loss factor is a function of layers and core thickness, the angles of the fibers, and the magnetic field intensity. The structure's mass is also affected by the thickness and density of layers and core. Therefore, the following relationships represent the mathematical expression of design variables and objective functions:

$$\text{Modal loss factor} = f(\theta_{t1}, \theta_{t2}, \theta_{t3}, h_t, h_c, B) \quad (18)$$

$$\text{mass} = f(h_t, h_c, \rho_t, \rho_c) \quad (19)$$

The range of changes related to the thickness (thickness of the whole panel) is consistently between 2 and 10 mm.

The angles of the fibers can also be changed between - 90 and + 90 degrees with a value of 2 degrees discretely.
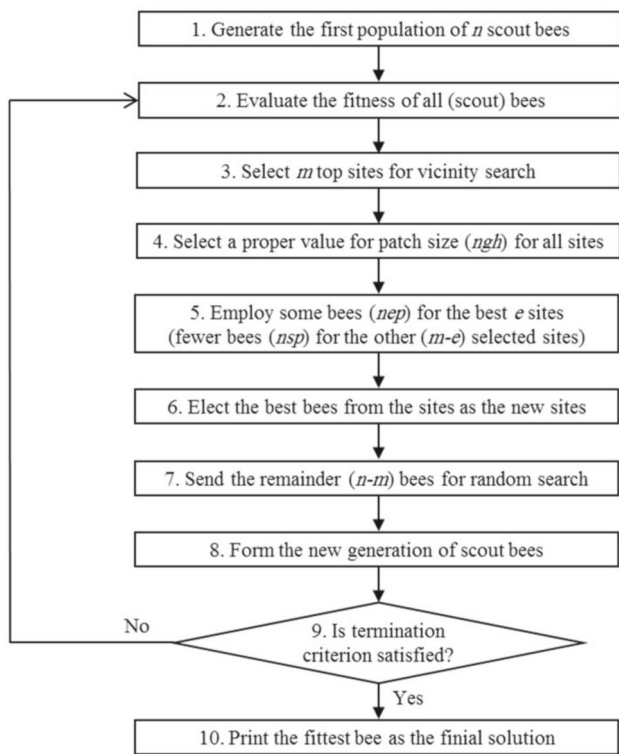
Fig. 2 The proposed flowchart for the basic bee algorithm

Table 1 Parameters in the bee algorithm

Parameter	Definition
n	Number of the Scout bee
m	Number of groups, excluding the random group
i	Group index
j	Input variable index
Ngh	Radius vector of the neighborhood
Ngh(i)	Radius vector of the neighborhood

The intensity of the magnetic field can also vary between 0 and 500 gausses with an increase of 10 G. discretely. For multi-objective optimization, the population size used in the proposed method and particle swarm optimization algorithm is 150.

4 Results

The aim of this section is to associate the numerical results obtained in this study with those obtained in other studies of a similar nature. According to Table 2, the results of the present research using the IHOT of sandwich panels have been matched with those obtained via the high-order theory of sandwich panels (Biglari and Jafari 2010). Similarly, in

Table 2 Values of natural frequencies for the sandwich panel

Natural frequency (Hz)	Present method	Ref. Biglari and Jafari (2010)	Error (%)
First	14.42	14.59	1.17
Second	25.69	26.86	4.36
Third	27.09	27.35	0.95
Fourth	35.16	35.54	1.07

Table 3 Optimum values for the sandwich panel with MR core

Parameter	Present method	Ref. Asgari (2010)	Error (%)
h_l (mm)	0.19	0.20	5.00
h_c (mm)	1.89	2.00	5.50
m (kg)	0.449	0.484	7.23
Modal damping ratio	0.125409	0.13722	8.61

Table 3, the optimization results obtained from this research using the bee algorithm method are compared with those acquired from particle swarm (Asgari 2010) and genetic algorithms. Table 2 demonstrates a respectable agreement between the results, which indicates the certainty and accuracy of the equations extracted in the present research. The lack of complete compatibility is due to the difference in the solution method. In addition, in the high-order theory of sandwich panels, the classical theory of multi-layered panels is used for the layers, and the vertical and transverse shear strains of the layers are omitted. In Table 3, the energy loss factor was compared with the existing results of ref. (Asgari 2010). The results show that the accuracy of the current study is around 8%, and one of the factors of this error is related to the different theories used and the solution method.

Subsequently, two single-objective and two-objective optimization problems have been investigated.

4.1 Maximization of the first loss factor of the sandwich panel considering the mass constraint

In this example, a symmetrical doubly-curved composite panel with composite layers consisting of three layers with a thickness equal to h_l and an MR core with a thickness of h_c is designed to maximize the loss factor by considering the mass constraint. The maximum weight of the panel is considered 500 g. This problem is also solved by the bee algorithm, and Fig. 3 illustrates the most optimal values of the modal loss factor in terms of generations. As shown in Fig. 3, from generation 45 onwards, the optimal value of the objective
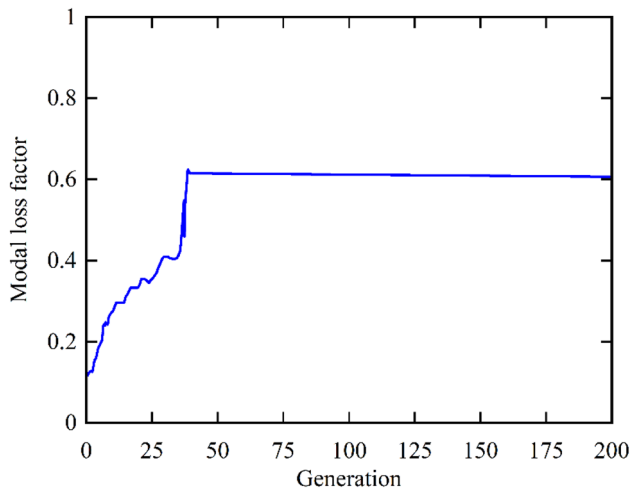
Fig. 3 Convergence diagram of a modal mass factor in terms of generations for the single-objective mode of doubly-curved sandwich panel
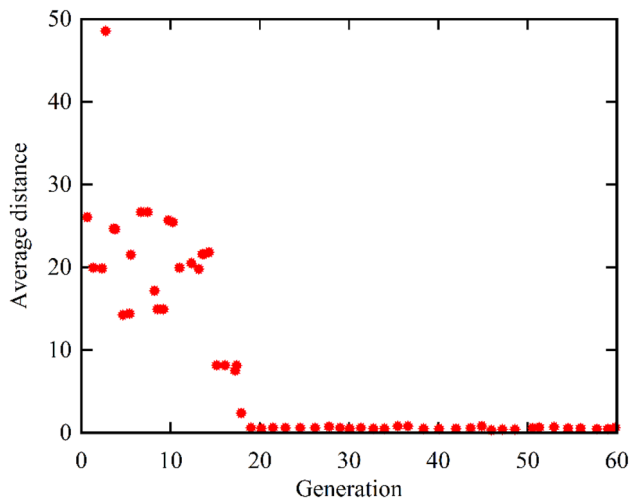
Table 4 Optimal parameters and the objective function for a single-objective mode of the doubly-curved panel

Parameters and objective function	Value
h_l (mm)	0.423
h_c (mm)	1.982
$\theta_{t1} = \theta_{b3}$	$-69°$
$\theta_{t2} = \theta_{b2}$	$24°$
$\theta_{t3} = \theta_{b1}$	$60°$
B (G)	0.859
m (kg)	0.429
Modal loss factor	0.152348

Fig. 4 The average distance in each generation in the single-objective mode of the doubly-curved sandwich panel

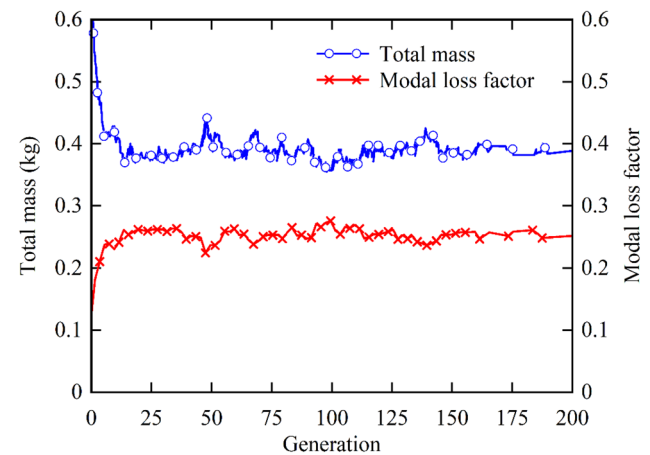**Fig. 5** Convergence diagram of structural mass and modal loss factor in the two-objective mode of doubly-curved sandwich panel

function has not changed. In other words, convergence has begun, and the average and best points have coincided. And finally, it has reached an end in the 55th generation of the algorithm. Figure 4 illustrates the average distance between generations. The distance is greater in the first generations and decreases as we approach the last generations. Finally, the optimal values for the variables and the objective function for this problem are presented in Table 4.

4.2 Optimization of the doubly-curved sandwich panel for maximum modal loss factor and minimum mass

In this case, the aim is to obtain optimal solutions of the Pareto front for the maximum loss factor and the minimum mass for

the doubly-curved sandwich panel. The design parameters, like the previous problems, include magnetic field intensity, fiber angles, the thickness of composite layers, and core thickness. Figure 5 shows the average distance between individuals in each generation. In this case, as can be observed, the distance is greater in the first generations and decreases as we approach the last generations. Figure 6 depicts the Pareto front. As mentioned earlier, it is observable that the optimal solutions are obtained as a set of points that form a front. One can choose among the optimal answers based on the need since none of the answers is optimal in the absolute sense.

In this problem, the TOPSIS method has been utilized to select a design point among the Pareto front points (Shih and Olson 2022). Based on this, point number 10 was selected as the design point, and the optimal values of the parameters and the objective function at this point are provided in Table 5. Figure 7 shows the convergence diagram. Also, the convergence results of the proposed method, and the particle swarm optimization algorithms are given for comparison. As can be detected, the proposed algorithm achieved the optimal design
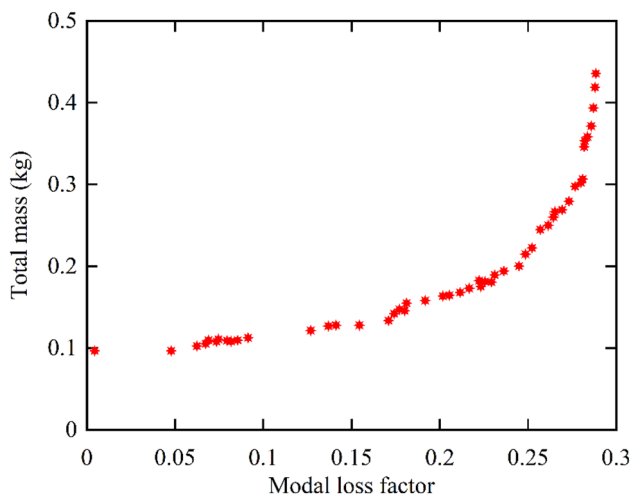
Fig. 6 Pareto front for the two-objective mode of a doubly-curved sandwich panel

Table 5 Optimal values of parameters and objective function for two-objective optimization

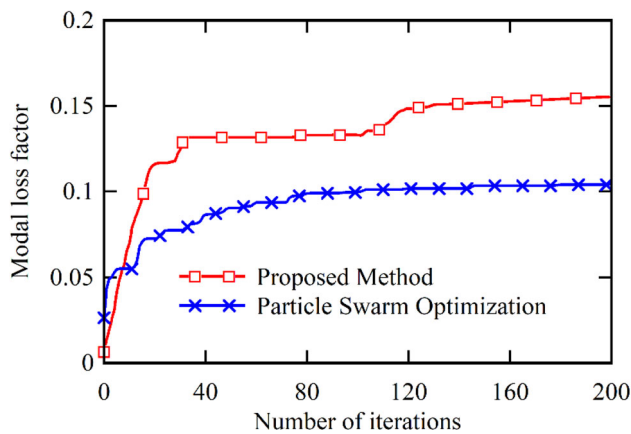| Parameters and objective function	Proposed method	Particle Swarm Optimization
hl (mm)	0.408	0.412
hc (mm)	1.396	1.238
$\theta_{t1} = \theta_{b3}$	$-46°$	85
$\theta_{t2} = \theta_{b2}$	$-32°$	40
$\theta_{t3} = \theta_{b1}$	$80°$	-32
B (G)	3.56	4.15
m (kg)	0.1268	0.185
Modal loss factor	0.154468	0.102354
Computational time (s)	32.42	35.65

Fig. 7 Convergence diagram of modal loss factor of the proposed method, and the particle swarm optimization

in less than 150 iterations. However, the computational time needed to achieve the optimal results of the proposed method is much less than that of particle swarm optimization.

5 Conclusion

Overall, in the current research, the thickness layers, angles of the fibers, and the magnetic field intensity are deliberated as optimization variables. Additionally, the maximum modal loss factor in the single-objective mode and the maximum modal loss factor, and the minimum mass in the dual-objective mode (with the functions of the mass objective and the modal loss factor) for sandwich panel with composite layers and MR core were analyzed. In the single-objective mode, the optimal values have been acquired, and in the multi-objective mode of the Pareto front, the optimal solutions have been presented. Regarding the single-objective mode, the results indicate the tendency of the structure to have thin layers and a thick core, which appears correct and feasible from a physical point of view, as MR fluid is placed in the core and contributes significantly to the increase in the modal loss factor. In the two-objective mode, the optimal solutions are obtained as a set of points that form a front. In fact, none of the resulting answers is optimal, and one of these optimal answers can be chosen depending on the need. Ultimately, in the case of the two-objective mode, TOPSIS was utilized to select a design point from the points of the Pareto front and to determine optimal values of parameters and objective functions.

The proposed approach may be extended in future research to identify optimal designs of curved sandwich panels by taking dynamic failure mechanisms into consideration in the optimization process. Moreover, further research will be conducted to increase the strength of sandwich panels. The proposed optimization algorithms still have a great deal of potential for speeding up. Additionally, artificial intelligence or machine learning methods may also play an important role in optimizing the performance of doubly-curved sandwich panels. Further work should focus on these meaningful topics.

Declarations

References

Asgari M (2010) Optimum design of composite sandwich panels with Magneto-Rheological fluid layer using new high order theory. M.Sc. Thesis, Department of Aerospace Engineering, KN Toosi University

Biglari H, Jafari AA (2010) High-order free vibrations of doubly-curved sandwich panels with flexible core based on a refined three-layered theory. Compos Struct 92(11):2685–2694

Boddeti N, Tang Y, Maute K, Rosen DW, Dunn ML (2020) Optimal design and manufacture of variable stiffness laminated continuous fiber reinforced composites. Sci Rep 10(1):16507

Cai S, Zhang P, Dai W, Cheng Y, Liu J (2021) Multi-objective optimization for designing metallic corrugated core sandwich panels under air blast loading. J Sandwich Struct Mater 23(4):1192–1220

Fallah M, Arab Maleki V (2021) Piezoelectric energy harvesting using a porous beam under fluid-induced vibrations. Amirkabir J Mech Eng 53(8):4633–4648

Frostig Y, Thomsen OT (2004) High-order free vibration of sandwich panels with a flexible core. Int J Solids Struct 41(5–6):1697–1724

Gao F, Sun W, Gao J (2019) Optimal design of the hard-coating blisk using nonlinear dynamic analysis and multi-objective genetic algorithm. Compos Struct 208:357–366

Hoseinzadeh M, Pilafkan R, Maleki VA (2023) Size-dependent linear and nonlinear vibration of functionally graded CNT reinforced imperfect microplates submerged in fluid medium. Ocean Eng 268:113257

Joladarashi S, Nagiredla S, Kumar H (2022) Characterization of an in-house prepared MR fluid and vibrational behaviour of composite sandwich beam with MR fluid core. Sci Iran. https://doi.org/10.24200/sci.2022.58527.5777

Kamaruddin S, Abd Latif MAH (2019) Application of the bees algorithm for constrained mechanical design optimisation problem. Int J Eng Mater Manuf 4(1):27–32

Khosravi F (2022) The post-buckling analysis of porous sandwich cylindrical shells with shape memory alloy wires reinforced layers under mechanical loads. Int J Appl Mech 14(6):2250064

Kolekar S, Venkatesh K, Oh J-S, Choi S-B (2019) Vibration controllability of sandwich structures with smart materials of electrorheological fluids and magnetorheological materials: a review. J Vibr Eng Technol 7:359–377

Li B, Gong Y, Gao Y, Hou M, Li L (2022) Failure analysis of hat-stringer-stiffened aircraft composite panels under four-point bending loading. Materials 15(7):2430

Lotfan S, Anamagh MR, Bediz B (2021) A general higher-order model for vibration analysis of axially moving doubly-curved panels/shells. Thin-Walled Struct 164:107813

Ly DK, Truong TT, Nguyen-Thoi T (2022a) Multi-objective optimization of laminated functionally graded carbon nanotube-reinforced composite plates using deep feedforward neural networks-NSGAII algorithm. Int J Comput Methods 19(03):2150065

Ly D-K, Truong TT, Nguyen S-N, Nguyen-Thoi T (2022b) A smoothed finite element formulation using zig-zag theory for hybrid damping vibration control of laminated functionally graded carbon nanotube reinforced composite plates. Eng Anal Boundary Elem 144:456–474

Ly K-D, Nguyen-Thoi T, Truong TT, Nguyen S-N (2022c) Multi-objective optimization of the active constrained layer damping for smart damping treatment in magneto-electro-elastic plate structures. Int J Mech Mater Des 18(3):633–663

Makweche D, Dundu M (2022) A review of the characteristics and structural behaviour of sandwich panels. Proc Inst Civil Eng Struct Build 175(12):965–979

Maleki VA, Mohammadi N (2017) Buckling analysis of cracked functionally graded material column with piezoelectric patches. Smart Mater Struct 26(3):035031

Maleki FK, Toygar ME (2019) The fracture behavior of sandwich composites with different core densities and thickness subjected to mode I loading at different temperatures. Mater Res Expr 6(4):045314

Maleki FK, Nasution MK, Gok MS, Maleki VA (2022) An experimental investigation on mechanical properties of Fe_2O_3 microparticles reinforced polypropylene. J Market Res 16:229–237

Mirzavand Borojeni B, Shams S, Kazemi MR, Rokn-Abadi M (2022) Effect of temperature and magnetoelastic loads on the free vibration of a sandwich beam with magnetorheological core and functionally graded material constraining layer. Acta Mech 233(11):4939–4959

Momeni S, Zabihollah A (2023) Effects of base material and magnetic field on the dynamic response of MR-laminated composite structures. Mech Based Des Struct Mach. https://doi.org/10.1080/15397734.2023.2201616

Nagiredla S, Joladarashi S, Kumar H (2022) Combined damping effect of the composite material and magnetorheological fluid on static and dynamic behavior of the sandwich beam. J Vibr Eng Technol 11(5):2485–2504

Nagiredla S, Joladarashi S, Kumar H (2023) Influence of material and geometrical properties on static and dynamic behavior of MR fluid sandwich beam: finite element approach. Iran J Sci Technol Trans Mech Eng. https://doi.org/10.1007/s40997-023-00603-7

Nasrabadi M, Sevbitov AV, Maleki VA, Akbar N, Javanshir I (2022) Passive fluid-induced vibration control of viscoelastic cylinder using nonlinear energy sink. Mar Struct 81:103116

Nguyen-Thoi T, Ly K-D, Truong TT, Nguyen S-N, Mahesh V (2022) Analysis and optimal control of smart damping for porous functionally graded magneto-electro-elastic plate using smoothed FEM and metaheuristic algorithm. Eng Struct 259:114062

Niu Y, Yao M, Wu Q (2022) Nonlinear vibrations of functionally graded graphene reinforced composite cylindrical panels. Appl Math Model 101:1–18

Pekbey Y, Maleki FK, Yildiz H, Hesar GG (2012) The meshless element free Galerkin method for buckling analysis of simply supported laminate composite plates. Adv Compos Lett 21(6):096369351202100602

Pham DT, Ghanbarzadeh A, Koç E, Otri S, Rahim S, Zaidi M (2006) The bees algorithm—a novel tool for complex optimisation problems. Intelligent production machines and systems. Elsevier, Amsterdam, pp 454–459

Pourreza T, Alijani A, Maleki VA, Kazemi A (2021) Nonlinear vibration of nanosheets subjected to electromagnetic fields and electrical current. Adv Nano Res 10(5):481

Pourreza T, Alijani A, Maleki VA, Kazemi A (2022) The effect of magnetic field on buckling and nonlinear vibrations of Graphene nanosheets based on nonlocal elasticity theory. Int J Nano Dimension 13(1):54–70

Rajamohan V, Sedaghati R, Rakheja S (2010) Optimum design of a multilayer beam partially treated with magnetorheological fluid. Smart Mater Struct 19(6):065002

Rezaee M, Arab Maleki V (2019) Passive vibration control of the fluid conveying pipes using dynamic vibration absorber. Amirkabir J Mech Eng 51(3):111–120

Rezaee M, Maleki VA (2015) An analytical solution for vibration analysis of carbon nanotube conveying viscose fluid embedded in visco-elastic medium. Proc Inst Mech Eng C J Mech Eng Sci 229(4):644–650

Sahu SK, Sreekanth PR, Reddy SK (2022) A brief review on advanced sandwich structures with customized design core and composite face sheet. Polymers 14(20):4267

San Ha N, Lu G (2020) A review of recent research on bio-inspired structures and materials for energy absorption applications. Composites B Eng 181:107496

Selvaraj R, Subramani M, Ramamoorthy M (2023) Vibration characteristics and optimal design of composite sandwich beam with partially configured hybrid MR-Elastomers. Mech Based Des Struct Mach 51(4):2200–2216

Sharif U, Chen L, Sun B, Ibrahim DS, Adewale OO, Tariq N (2022) An experimental study on dynamic behaviour of a sandwich beam with 3D printed hexagonal honeycomb core filled with magnetorheological elastomer (MRE). Smart Mater Struct 31(5):055004

Shih H-S, Olson DL (2022) TOPSIS and its extensions: a distance-based MCDM approach, vol 447. Springer Nature, Cham

Srinivasa N, Gurubasavaraju T, Kumar H, Arun M (2020) Vibration analysis of fully and partially filled sandwiched cantilever beam with magnetorheological fluid. J Eng Sci Technol 15(5):3162–3177

Toygar ME, Tee KF, Maleki FK, Balaban AC (2019) Experimental, analytical and numerical study of mechanical properties and fracture energy for composite sandwich beams. J Sandwich Struct Mater 21(3):1167–1189

Vinyas M (2020) On frequency response of porous functionally graded magneto-electro-elastic circular and annular plates with different electro-magnetic conditions using HSDT. Compos Struct 240:112044

Zhao J, Fan G, Guan J, Li H, Gao Z, Ma H (2023) Dynamic analyses of composite corrugated sandwich plates filled with magnetorheological elastomer resting on elastic foundation. Eng Struct 289:116229

Zheng W, Liu J, Oyarhossein MA, Safarpour H, Habibi M (2023) Prediction of nth-order derivatives for vibration responses of a sandwich shell composed of a magnetorheological core and composite face layers. Eng Anal Boundary Elem 146:170–183